RANGING IN THE IEEE 802.15.4A STANDARD USING ENERGY DETECTORS

Bernhard Geiger, *Student Member*

***Abstract*—Ranging is strongly dependend of an accurate estimation of time-of-arrival (TOA), which requires fine temporal resolution. Ultrawide band (UWB) pulses fulfill this requirement, but the pulses are spread in time by multipath propagation. The major concern in ranging therefore is a proper detection of the leading edge. The IEEE 802.15.4a standard defines a way of TOA-based ranging with coding gain by exploiting a series of ternary preamble sequences with perfect autocorrelation properties. The focus of this work is on the implementation of a standard compliant ranging method, as well as on simulations evaluating the performance of energy detectors applying this method.**

***Index Terms*—Ultra wideband communications, IEEE 802.15, energy detector, distance measurement**

I. INTRODUCTION

The high time resolution of UWB pulses is the main advantage of ranging capable devices (RDEVs), but they suffer from constricted power consumption due to reasons of mobility and from strict regulations concerning the maximum power level. Thus, these devices have to operate with reasonably low SNR values. The only possibility to maintain communication or acquisition is to artificially increase this SNR by introducing processing gain. Therefore, the IEEE 802.15.4a standard defines appropriate measures for communications (time-hopping to avoid multi-user interference, scrambling to increase coding gain) and ranging (ternary preamble sequences) [1].

Pulse-based ranging, which does not exploit coding gain, was a field of interest for many researchers [2]–[4]. This may come from the fact that the major concern in ranging – the detection of the leading edge – is so fundamental that it must be considered in any kind of ranging method. The literature derived from these considerations thus contains numerous ranging methods, from maximum energy selection (MES, [3]) over (weighted) maximum energy sum selection [5] to threshold comparison and search-back algorithms (TC, MES-SB, [3], [4]). Threshold selection methods were introduced as well [2]–[6]. Sub-meter ranging was achieved in regions with high SNR values by low-power, low-complexity receivers.

Ranging with coding gain appeared about the same time in literature. The focus of these works was mainly put on increasing the coding gain by using preamble sequences with perfect autocorrelation properties [6]–[8]. An enormous increase in performance was achieved in terms of SNR requirements. Sub-meter ranging was now possible with much lower SNR values due to high coding gain. Consequently, leading edge detection techniques were reduced to simple threshold comparison or search-back algorithms with constant false alarm rates [6]. This work on the other hand tries to apply leading edge detection techniques developed for pulse-based ranging on ranging with coding gain, i.e. with ternary preamble sequences.

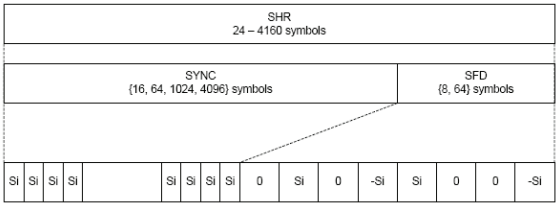

Fig. 1 – Synchronisation header structure [1]

The paper is organized as follows: Section II gives an overview of the ranging features of the IEEE 802.15.4a, especially of the synchronisation preamble. Section III is devoted to general considerations about the applied channel model and energy detectors. The following Section IV discusses power delay profile estimation and introduces a variety of ranging algorithms. Finally, Section V compares ranging performance of different preamble parameters and illustrates simulation results.

II. IEEE 802.15.4A RANGING

Every packet transmission includes a synchronisation header (SHR, see Fig. 1), which itself contains a portion especially designed for synchronisation purposes (SYNC) and a portion signalling the end of the SHR and the beginning of the PHY header, namely the *start-of-frame* delimiter (SFD). Each of these portions is built up of ternary preamble sequences with perfect autocorrelation properties. How they are constructed in detail will be discussed in the following subsections.

A. Ternary Preamble Sequences (TPS)

In order to enable synchronisation and ranging, standard compliant devices are provided with a set of 24 ternary code sequences $\mathbf{C}_i$. The first eight code sequences $\mathbf{C}_1$ to $\mathbf{C}_8$ are length $N_{code} = 31$ (see Tab. I), the remaining 16 codes have a length of $N_{code} = 127$. All of them share perfect cyclic autocorrelation, in other words, the cyclic autocorrelation sequence does not suffer from side lobes [9]. As an example, the ternary code sequence $\mathbf{C}_1$ and its cyclic autocorrelation can be seen in Fig. 2. This

978-1-4244-3861-7/09/$25.00 ©2009 IEEE

perfect autocorrelation allows simple channel inpulse response (CIR) or power delay profile (PDP) estimation, depending on the type of receiver used.

Additionally, the codes share sub-optimum cross-correlation properties, meaning that autocorrelation outstands cross-correlation by far in most of the cases. Within one particular channel, only those code sequences $\mathbf{C}_i$ may be used which have the lowest cross-correlation in order to reduce multi-user interference to a minimum (see Tab. I) [1].

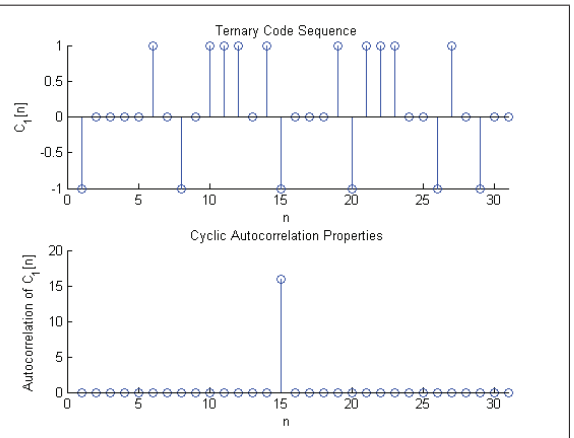

Fig. 2 – Ternary Code and Cyclic Autocorrelation

Table I. Ternary Codes with length $N_{code} = 31$ [1]

i	$\mathbf{C}_i$	Channel Number
1	-0000+0-0+++0+-000+-+++00-+0-00	0,1,8,12
2	0+0+-0+0+000-++0-+—00+00++000	0,1,8,12
3	-+0++000-+-++00++0+00-0000-0+0-	2,5,9,13
4	0000+-00-00-++++0+-+000+0-0++0-	2,5,9,13
5	-0+-00+++-+000-+0+++0-0+0000-00	3,6,10,14
6	++00+00—+-0++-000+0+0-+0+0000	3,6,10,14
7	+0000+-0+0+00+000+0++—0-+00-+	4,7,11,15
8	0+00-0-0++0000–+00-+0++-++0+00	4,7,11,15

A low-power way of generating these preamble sequences using linear feedback shift registers can be found in [7].

B. Spreading and Zero Padding

In order to get one preamble symbol $\mathbf{S}_i$, the ternary code sequence $\mathbf{C}_i$ must be spread by a delta function δ_L of length L, which is chosen according to the pulse repetition frequency (PRF) [1],

$$\mathbf{S}_i = \mathbf{C}_i \otimes \delta_L[n] \tag{1}$$

where $\otimes$ denotes the Kronecker product and

$$\delta_L[n] = \begin{cases} 1 & n = 0 \\ 0 & n = 1..L-1 \end{cases} . \tag{2}$$

While for TPS with $N_{code} = 127$ the spreading length is always $L = 4$, there are two possible PRFs for the short sequences, namely $L = 16$ (corresponding to the high PRF) and $L = 64$ (low PRF). This is governed by the fact that the devices will operate in environments with widely varying delay spreads. By spreading the code sequence we get the following relation for the number of chips N_C per preamble symbol:

$$N_C = N_{code} L \tag{3}$$

C. Symbol Repetition

The preamble symbol $\mathbf{S}_i$ is then repeated in order to generate the SYNC field of the SHR. The number of symbol repetitions are $N_{sync} = \{16, 64, 1024, 4096\}$ making four possible durations of the SHR [1]. Mathematically, the SYNC portion can be constructed as follows:

$$\mathbf{M}_i = \delta_N[n] \otimes \mathbf{S}_i \tag{4}$$

with

$$\delta_N[n] = \begin{cases} 1 & n = 0..N_{sync}-1 \\ 0 & elsewhere \end{cases} . \tag{5}$$

Which of these lengths is chosen strongly depends on the power delay profile of the channel, the capabilities of the RDEVs and the SNR of the link. Especially the longer preamble lengths (1024 and 4096) are used for non-coherent receivers, since they can improve the SNR via processing gain [9]. However, it is suggested that every device starts ranging with the *medium* symbol repetition number of $N_{sync} = 1024$. Further adjustment of preamble length can be done by keeping track of the SNR, i.e. increasing or decreasing preamble lengths with decreasing or increasing SNR.

The SYNC signal $s_i(t)$ is obtained by modulation of the UWB pulse waveform $\phi(t)$, a root-raised cosine (RRC) filtered delta pulse,

$$s_i(t) = \sqrt{\frac{E_S}{N_N}} \sum_{n=0}^{N_C N_{sync}-1} \mathbf{M}_i[n]\phi(t - nT_C), \tag{6}$$

where E_S is the symbol energy and N_N the number of non-zero chips per symbol. The synchonisation symbol $s_i(t)$ has a duration described by the following equation:

$$T_{sync} = N_C N_{sync} T_C \tag{7}$$

Assuming that the chip duration $T_C \approx 2ns$, one can show that depending on the configuration T_{sync} can be as short as 16 μs, but it can be up to 4.1 ms as well. Here another problem may arise: In terms of power delay profile estimation it cannot be granted that the CIR stays constant over such a long period. Still, for the sake of simplicity a constant CIR is assumed in this paper.

III. Channel Model and Energy Detection

A. Channel Model

Every radio system suffers from multipath propagation. UWB systems show less small scale fading, therefore they are more robust than narrow band systems. In fact, using UWB systems even single multipath components can be resolved. The CIR can

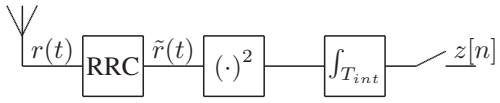

Fig. 3 – Energy Detector

be approximated by a series of weighted delta-pulses, namely

$$h(t) = \sum_{l=0}^{L_{mp}} \alpha_l \delta(t - \tau_l), \tag{8}$$

where L_{mp} is the number of multipath components (MPC), α_l the (complex) path gain and τ_l the path delay of the l-th MPC [10]. By convolving the CIR with the UWB pulse waveform we get the received pulse waveform $\phi_{mp}(t)$

$$\phi_{mp}(t) = \sum_{l=0}^{L_{mp}} \alpha_l \phi(t - \tau_l). \tag{9}$$

It is well known that not always the strongest pulse is identical to the leading pulse, especially in non-line-of-sight (NLOS) environments. The major challenge in ranging therefore is the detection of the leading edge of the CIR. The actual channel model used in this paper was introduced in [11]. Its average power delay profile $P_h(t)$ is characterized by an exponential decay,

$$P_h(t) = \frac{E_h}{\tau_{RMS}} e^{-\frac{t}{\tau_{RMS}}}, \tag{10}$$

where E_h is the average received energy and τ_{RMS} the root-mean square delay spread. The fourth-order function $R_h(t)$ characterizes the ray arrival times and the ray amplitude statistics. The arrival times are uniformly Poisson-distributed with a rate of $\bar{\lambda}$ rays per second, whereas the ray amplitudes are Nakagami-m distributed. Hence

$$R_h(t) = P_h^2(t) \left(1 + \frac{1}{m}\right) \frac{1}{\bar{\lambda}}. \tag{11}$$

The fact, that MPCs arrive in clusters according to the Saleh-Valenzuela model [12] is neglected in this model.

B. Energy Detector

The main advantage of energy detectors (EDs, see Fig. 3) is that they do not require Nyquist sampling rates, which can be up to 60 GHz due to short pulse durations [1]. Instead, a receiver using energy detection first filters the received signal with an RRC filter. Since the received pulse shape is a RRC-filtered delta pulse itself, the output of the bandpass filter is a raised-cosine (RC) filtered delta pulse:

$$\tilde{r}(t) = \sqrt{\frac{E_S}{N_N}} \sum_{n=0}^{N_C N_{sync}-1} \mathbf{M}_i[n] \Phi_{mp}(t - nT_C) + \tilde{n}(t), \tag{12}$$

where $\tilde{n}(t)$ is the RRC-filtered complex Gaussian zero-mean noise, and $\Phi_{mp}(t)$ is the RC-filtered CIR (often referred to as compound impulse response). This signal now is the input to a square law device, whose output is then integrated and sampled:

$$z[n] = \int_{(n-1)T_{int}}^{nT_{int}} \tilde{r}^2(t) dt \tag{13}$$

The obtained samples $z[n]$ obviously represent the collected energy between the time instants $(n-1)T_{int}$ and nT_{int}. It is noteworthy that some of these samples contain noise energy only, whereas only the minority of samples contain the actual signal. Additionally, the signal energy is distributed over the delay spread of the CIR due to multipath propagation.

IV. Ranging using TPS

Since leading edge detection is a problem for all ranging methods disregarding whether they take advantage of ternary preamble sequences or not most of the literature covers simple pulse-wise ranging methods. Some of the literature however reports about increased performance due to the use of TPS in ranging [6]–[8], [13]. Although these works implement the TPSs defined in the IEEE 802.15.4a standard, they do not take care of any standard compliancy (with respect to timing parameters or zero spreading). In fact, a standard compliant SHR used for ranging cannot be found in the literature. Therefore, the focus of this work was put on ranging simulations with a standard compliant SHR.

A significant problem with ranging with EDs arises from the finite length of the integration interval T_{int} or - equivalently - from sub-Nyquist sampling. Assuming that the position of leading edge is uniformly distributed within one sampling period, the mean absolute error (MAE) is at least $\frac{T_{int}}{4}$, if the position of the leading edge is estimated at the center point of the integration interval [3]. Thus, shorter integration intervals (or higher sampling rates, respectively) lead to less MAE.

On the other hand, shorter integration intervals lead to an increased number of blocks with less energy in each block. Additionally to the subsequently increased memory and processing power the probability for a false detection increases as well [3].

This part of the document explains how the PDP can be estimated using TPS and how this estimation can be exploited for estimating the TOA. Furthermore, a variety of ranging methods is introduced (see Fig. 4).

A. Power Delay Profile (PDP) Estimation

After integration the energy values are stored in a shift register, which should contain at least one preamble symbol. In other words, given an integration interval T_{int}, the minimum register length would be

$$N_{reg} = \frac{N_{code} L T_C}{T_{int}}. \tag{14}$$

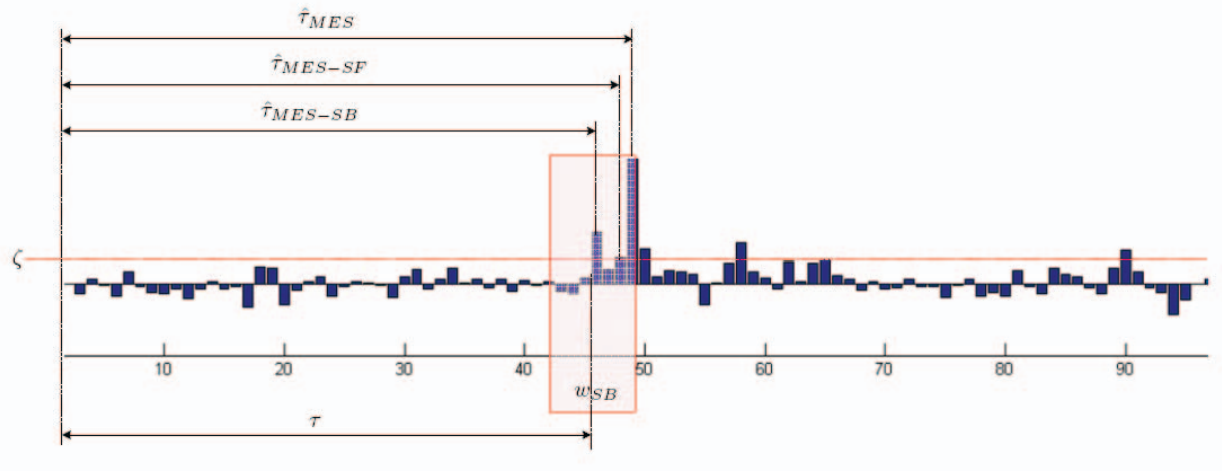

Fig. 4 – Different methods of TOA estimation (using TPS)

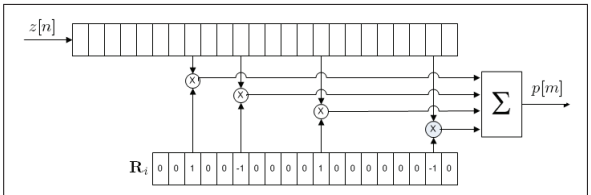

Fig. 5 – Sliding window correlator for PDP estimation

This shift register feeds a sliding-window correlator (see Fig. 5), which contains the reference preamble sequence $\mathbf{R}_i$ for means of cross-correlation. This sequence is – similar to the original preamble symbol $\mathbf{S}_i$ – obtained from the ternary code sequences $\mathbf{C}_i$. However, in order to preserve the perfect autocorrelation properties, the reference symbol has to be defined as follows [7]: First, the ternary code sequence $\mathbf{C}_i$ has to be converted to a binary zero-mean code sequence. This is accomplished by taking the absolute value of each code (so that all active codes are 1) and then setting all non-active codes to -1. If, as a second possibility, the non-active codes are set to $-\frac{16}{15}$ (or $-\frac{64}{63}$ for the long preamble codes) a zero-mean code is obtained by sacrifizing perfect autocorrelation properties. While the zero-mean code will have the advantage of less noise accumulation, it will suffer from non-zero side lobes. Which of these options is preferable is within the scope of future work. In any case, the obtained reference sequence has to be spread according to equation (1). The main advantage of a reference sequence constructed like this is that only N_{code} multiplications have to be done for each time lag, since due to spreading with zeros all other multiplications are zero.

A receiver using ED applies a square law device to the received signal. Therefore, the sequence of energy blocks $z[n]$ is non-negative and not zero-mean anymore. Consequently, if perfect autocorrelation is preserved instead of the cross-correlation between $z[n]$ and $R_i[n]$ (a sequence of values contained in $\mathbf{R}_i$) the covariance function has to be calculated, that is:

$$p[m] = \sum_{n=0}^{N_{reg}} R_i[n]\left(z[n-m] - \mu_z\right), \qquad (15)$$

where μ_z is the mean of all energy blocks stored in the shift register. Because of the perfect autocorrelation properties of the TPS and the well-constructed reference symbol $p[m]$ can be interpreted as a sampled version of the squared, RC-filtered CIR – the power delay profile (PDP) estimation. If, on the other hand the zero-mean reference symbol is chosen, the cross-correlation function can be used to estimate the PDP, now influenced by side-lobes:

$$p[m] = \sum_{n=0}^{N_{reg}} R_i[n] z[n-m] \qquad (16)$$

These estimations can then be averaged over N_{sync} synchronisation symbols in order to flatten the power spectral density of the squared noise signal. Stripping the mean value, which is automatically done by the covariance function or by the zero-mean reference sequence, leads to noise averaging and therefore increases ranging performance. Sub-optimal approaches may even apply cross-correlation to non zero-mean reference symbols, thus accumulating a certain amount of noise. If, and how such a simplification will influence ranging performance, is out of the scope of this paper.

B. Maximum Energy Selection (MES)

Maximum energy selection (MES) is by far the most simplistic, robust, and inaccurate way of ranging. From out of a series of integration blocks[1] $z[n]$ the one with the maximum energy value is assumed to contain

[1]For sake of simplicity I will refer to them as "peaks".

the leading edge and thus represents the estimate for the TOA [3]. Mathematically, this can be described by

$$\begin{aligned}\hat{\tau}_{MES} &= \left[\text{argmax}_n \{p[n]\} + \frac{1}{2}\right] T_{int} \\ &= \left[n_{max} + \frac{1}{2}\right] T_{int},\end{aligned} \tag{17}$$

where n_{max} is the index of the strongest peak and the center of the block was selected as TOA estimate. The index n is bounded and runs from $0..N_{reg}$.

Depending on the scenario the leading edge is not necessarily identical to the strongest peak and this method leads to big ranging errors. However, since only the strongest peak is selected, this method is relatively robust in low-SNR regions.

C. MES Search-Back (MES-SB)

MES search-back (MES-SB) uses a search-back window of length w_{SB} in front of the strongest peak. Thus, the leading edge most likely is placed within that window, and any threshold comparison can be constrained to this interval [3]. The first peak which exceeds the threshold ζ *within this window* is chosen as an estimate for the TOA. Mathematically,

$$\hat{\tau}_{MES-SB} = \left[\min_n \{n|\tilde{p}[n] > \zeta\} + n_{max} - w_{SB} - \frac{1}{2}\right] T_{int}, \tag{18}$$

where $\tilde{p}[n]$ collects all peaks within the search-back window,

$$\tilde{p}[n] = \Big[p[n_{max} - w_{SB}] \cdots p[n_{max}]\Big]. \tag{19}$$

In low-SNR regions the error can therefore be limited to the size of the search-back window, as long as the maximum energy block is detected correctly. Compared to the pure MES, leading edge detection is performed which significantly decreases the MAE, at least in regions with high SNR values.

In addition to threshold selection the size of the search-back window w_{SB} has to be selected based on signal statistics as well. Ref. [3] addresses this problem and states that the optimum window sizes are between 30 and 40 ns, for residental LOS and NLOS, respectively.

D. MES Search-Forward (MES-SF)

Another leading edge detection algorithm implemented in this work was an MES search-forward algorithm. After selecting the maximum energy peak, a search-back window of arbitrary length w_{SB} was chosen. Within this window the last peak *below* a certain threshold ζ was searched, and this peak was assumed to precede the leading edge immediately. The following peak therefore was selected as the estimated TOA, in other words

$$\hat{\tau}_{MES-SF} = \left[\max_n \{n|\tilde{p}[n] < \zeta\} + n_{max} - w_{SB} + \frac{1}{2}\right] T_{int}, \tag{20}$$

where $\tilde{p}[n]$ again contains the maximum energy peak and w_{SB} preceeding ones.

V. Simulations and Results

The following results were obtained by simulations over $N_{sim} = 500$ randomly generated channels according to the model presented in [11]. The root-mean square delay spread was set to $\tau_{RMS} = 5$ ns. Ray arrival and amplitude parameters were set to $\bar{\lambda} = 5\frac{1}{s}$ and $m = 1$. The integration interval was chosen from the set $T_{int} = \{1, 2, 4\}$ ns.

The mean absolute error (MAE) was calculated using the following relationship:

$$MAE = \frac{1}{N_{sim}} \sum_{k=0}^{N_{sim}-1} |\tau_k - \hat{\tau}_k|, \tag{21}$$

where τ_k is the actual and $\hat{\tau}_k$ the estimated TOA, depending on the ranging method.

The reference symbol $\mathbf{R}_i$ was designed to be zero-mean, thus sacrifizing perfect autocorrelation properties. PDP estimation was done using cross-correlation, implemented as matched filtering in the digital domain.

A. Maximum Energy Selection (MES)

As it was discussed earlier, there is a minimum MAE even if the correct energy block is selected, simply due to finite sampling rates. This MAE cannot be neglected for long integration periods of $T_{int} = 4$ ns. Any additional MAE in high-SNR regions stems from the fact that the peak path is not identical to the leading edge path, introducing an error proportional to the RMS delay spread. Comparatively high MAE in low-SNR regions can be explained by noise samples exceeding the correlation peak.

As it can be seen in Fig. 6 ranging performance increases with increasing number of symbol transmissions. This is caused by improved noise averaging and thus better PDP estimation. Not only the MAE is much lower for many symbol repetitions in low-SNR regions, also the correct strongest peak is selected at much lower SNR values.

Fig. 6 also shows the difference between different spreading lengths, $L = 16$ and $L = 64$ for the short preamble codes and $L = 4$ for the long ones. As it can be seen, longer spreading intervals cause greater MAE. This can be explained by the fact that with greater spreading intervals the number of samples within a symbol is increased and thus the probability for a false detection is much higher if the SNR is low. Additionally, the distance between the falsely detected peak and the actual strongest path is increased as well.

Looking at and Fig. 6 one may come to the conclusion that the performance of the long preamble symbol ($N_{code} = 127$) is slightly worse than the performance of the short ones. This might be caused by overlapping of the PDP due to short spreading

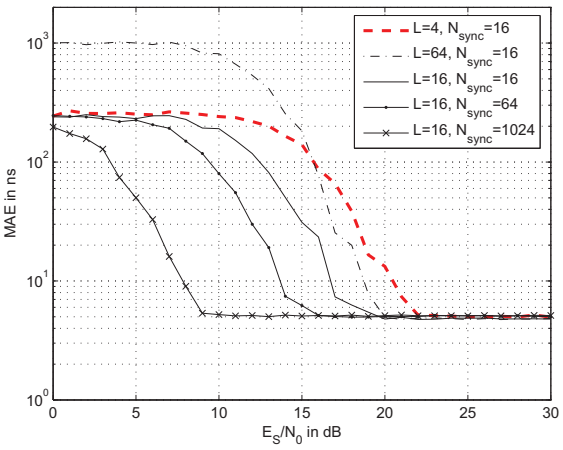

Fig. 6 – Ranging Performance for different preamble parameters (MES, $T_{int} = 2ns$)

intervals of only $L = 4$. What has to be taken into account is that the symbol energy is approximately four times as high as for the short preamble symbols.

The fact that the MAE exceeds 5 ns for the whole range of SNR explains why this method is not implemented in practice. In this work, however, it was mainly used for an easy comparison of different preamble parameters, such as symbol repetition count or spreading length.

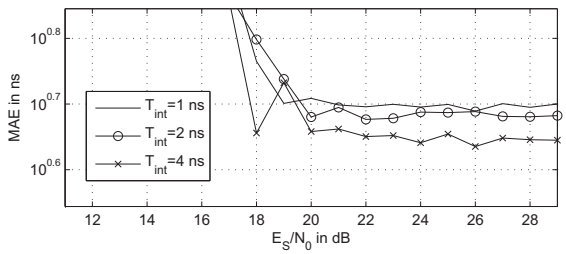

Fig. 7 – Influence of Integration Interval T_{int} (MES, L = 16, N_{sync} = 16)

A very interesting result is obtained from Fig. 7. As it can be seen, a short integration period of $T_{int} = 1$ ns results in larger error values in the high-SNR regions. This stems from the fact, that for high SNR values - which are necessary for accurate ranging - more high-energy blocks are in the close vincinity of the peak pulse[2]. Due to noise, these block may eventually exceed the peak. The increased number of blocks consequently increases the probability for a mis-detection and therefore results in higher MAE. Longer integration periods ($T_{int} = 4$ ns), on the other hand, reduce the number of possibilities for a mis-detection. Additionally, a single noise peak exceeding the maximum energy peak contributes less energy to the integration interval for longer values of T_{int}. The fact that long integration intervals outperform shorter ones is even more emphasized by taking into account that the minimum MAE increases with T_{int}.

[2]Recall the fact that the power delay profile is not the squared CIR, but the square of the RC-filtered CIR.

B. MES Search-Forward (MES-SF)

In these simulations a search-back window of length $w_{SB} = \left\lceil \frac{32}{T_{int}} \right\rceil$ was chosen. The threshold was set to its optimal value $\zeta = \zeta_{opt}$, which differs from one set of ranging parameters to another, but still can be determined without channel knowledge. As it can be seen in Fig. 8, the MAE in the high-SNR region ranges around 3 ns. The advantages and disadvantages of the chosen preamble parameters are identical to the ones described in the section about MES, i.e. a leading edge detection does not influence the ranging properties of the preamble or spreading lengths. Consequently, a higher number of symbol repetitions results in a smaller error for lower SNR values.

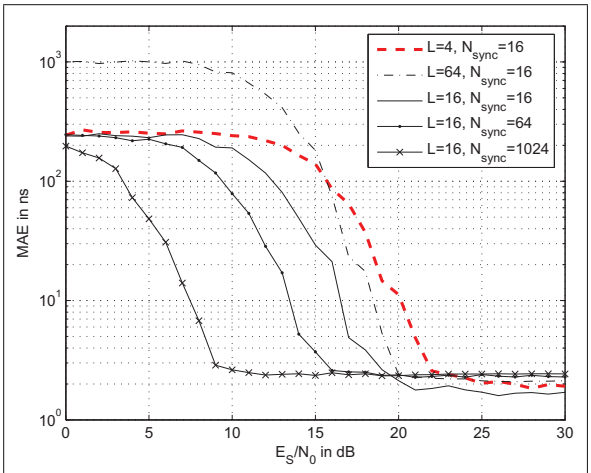

Fig. 8 – Ranging Results for different preamble parameters (MES-SF, $T_{int} = 2ns$)

C. MES Search-Back (MES-SB)

For the MES-SB algorithm the threshold again was set to its optimal value ζ_{opt}, which in this particular case not only depends on the ranging parameters L, N_{sync} and T_{int}, but also on the SNR. Fig. 9 illustrates the effect of different preamble parameters (compare to figures Fig. 6 and Fig. 8). As it can be seen, MAE values around and below 1 ns could be achieved, which is by far the best result in this series of simulations.

The main difference between MES-SF and MES-SB can be explained by looking at the channel models used in literature [14]. Due to pulse fading the RC-filtered CIR may contain a leading pulse which is followed by a zero interval. This interval finally is followed by the actual maximum energy pulse (constructive interference) and the decaying part of the CIR. While the MES-SB locks onto the leading pulse, MES-SF ignores this pulse and chooses the rise of the

maximum energy pulse as TOA estimate instead. This way, a greater mean absolute error is obtained.

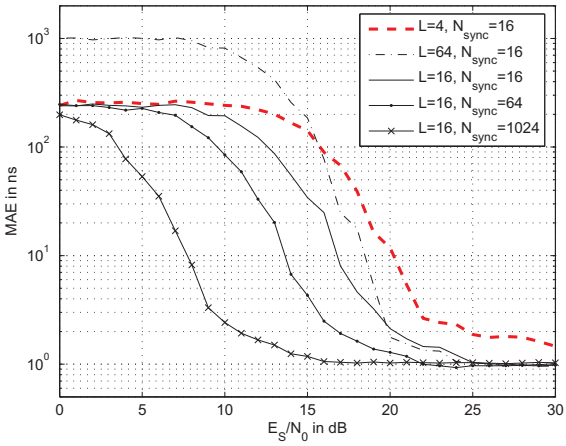

Fig. 9 – Ranging Results for different preamble parameters (MES-SB, $T_{int} = 2ns$)

Another interesting fact can be derived from a simulation run with different integration periods T_{int}. In contrast to MES, where longer integration intervals perform better in high-SNR regions, MES-SB yields better results when using short integration periods (see Fig. 10). This can be explained by looking at the search-back mechanism: Even if the maximum energy selection fails by choosing the wrong peak, the leading edge still can be detected correctly, if it is located within the search-back window. In order to accurately detect the leading edge, high temporal resolution is required - a requirement which can only be met by high-rate sampling, or short integration periods.

Fig. 11 summarizes the differences in ranging performance for MES, MES-SB and MES-SF. For this simulation, an integration period of $T_{int} = 1$ ns was used. It can be easily seen that, while all algorithms perform similarily in low-SNR regions, only the MES-SB achieves sub-nanosecond ranging for high SNR values. Yet, for thresholds independend of SNR, performance is reasonably decreased.

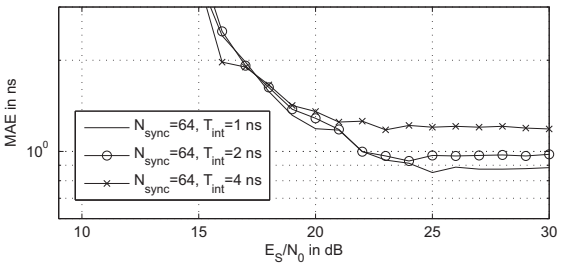

Fig. 10 – Comparison of different N_{sync} and T_{int} (MES-SB, L = 16, N_{sync} = 64)

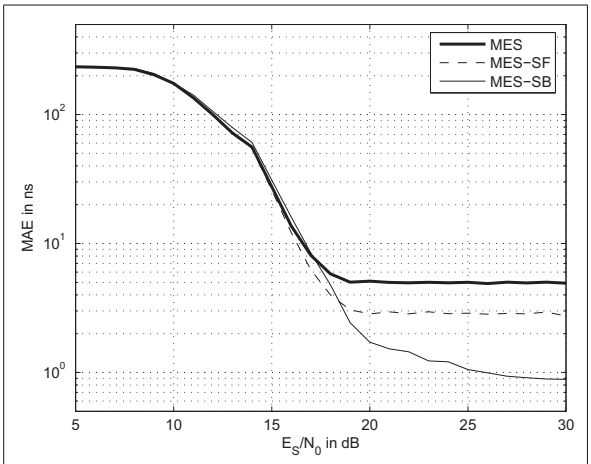

Fig. 11 – Comparison between different Ranging Algorithms (T_{int} = 1 ns, l = 16, N_{sync} = 64)

VI. Conclusion

As it can be seen in the illustrations, ranging with ternary preamble sequences achieves minimum error values. Leading edge detection techniques developed for pulse-based ranging can be applied for RDEVs compliant to the new standard. Additionally, the SNR requirements for ranging can be reduced significiantly by using higher numbers of symbol repetitions. Since energy detectors used for communications use much longer integration intervals to capture as much energy as possible, they cannot be applied for ranging with these settings unchanged. An energy detector which performs both ranging and communication with optimum energy consumption therefore has to adapt its integration interval according to the actual task.

Acknowledgements

The author would like to thank his supervisors Thomas Gigl, Graz University of Technology & CISC Semiconductor GmbH, and Klaus Witrisal, Graz University of Technology, for their fruitful suggestions and their support.

References

[1] "Approved draft amendment to ieee standard for information technology-telecommunications and information exchange between systems-part 15.4:wireless medium access control (mac) and physical layer (phy) specifications for low-rate wireless personal area networks (lr-wpans): Amendment to add alternate phy (amendment of ieee std 802.15.4)," August 2007.

[2] I. Guvenc and Z. Sahinoglu, "Threshold selection for UWB TOA estimation based on kurtosis analysis," *IEEE Communications Letters*, vol. 9, no. 12, pp. 1025–1027, December 2005.

[3] ——, "Threshold-based TOA estimation for impulse radio UWB systems," in *ICU 2005. IEEE International Conference on Ultra-Wideband.*, 09 2005.

[4] C. Xu and C. L. Law, "Experimental evaluation of UWB ranging performance for correlation and ED receivers in dense multipath environment," in *Future Generation Communication and Networking*, vol. 2, December 2007, pp. 186–192.
[5] I. Guvenc, Z. Sahinoglu, and P. V. Orlik, "TOA estimation for IR-UWB systems with different transceiver types," *IEEE Transactions on Microwave Theory and Techniques*, vol. 54, no. 4, pp. 1876–1886, April 2006.
[6] Z. Lei, F. Chin, and Y.-S. Kwok, "UWB ranging with energy detectors using ternary preamble sequences," in *WCNC*, 2006.
[7] Y.-S. Kwok, F. Chin, and X. Peng, "Ranging mechanism, preamble generation, and performance with IEEE 802.15.4a low-rate low-power UWB systems," in *IEEE Ninth Symposium on Spread Spectrum Techniques and Applications*, Sept. 2006, pp. 525–530.
[8] F. Chin, W. Zhi, and C.-C. Ko, "System performance of UWB based low rate wireless personal area network," in *Signals, Systems and Computers, 2003. Conference Record of the Thirty-Seventh Asilomar Conference on*, vol. 2, Nov. 2003, pp. 1235–1238 Vol.2.
[9] Z. Sahinoglu and S. Gezici, "Ranging in the IEEE 802.15.4a standard," in *Wireless and Microwave Technology Conference*, December 2006, pp. 1–5.
[10] I. Oppermann *et al.*, *UWB Theory and Application*. Chichester: John Wiley and Sons, Ltd, 2004.
[11] K. Witrisal and M. Pausini, "Statistical analysis of UWB channel correlation functions," *IEEE Transactions on Vehicular Technology*, vol. 53, no. 3, pp. 1359–1373, March 2008.
[12] A. Saleh and R. Valenzuela, "A statistical model for indoor multipath propagation," *IEEE Journal on Selected Areas in Communications*, vol. 5, pp. 128–137, 1987.
[13] K. Takizawa, H.-B. Li, and R. Kohno, "Precise leading edge detection using a forward error correction coding," in *Wireless Communication Systems*, Valencia, September 2006, pp. 734–738.
[14] J. Foerster *et al.*, *Channel modelling sub-committee report - Final*. IEEE P802.15 Working Group for Wireless Personal Area Networks (WPANs), 2003.

Bernhard Geiger (S' 07) finished Higher Technical College in 2003, Graz, and is currently studying Electrical Engineering with focus on Telecommunications at the Technical University of Graz. Presently, he is working on his MS thesis.

From 2007 to 2008 he was working as a study assistant at the Institute for Electrical Measurement and Measurement Signal Processing. Since 2007 he is also working as a study assistent at the Signal Processing and Speech Communication Laboratory.